Impact of Catalyst Geometry on Diffusion and Selective Catalytic Reduction Kinetics under Elevated Pressures

Daniel Peitz[1,2], Martin Elsener[3], and Oliver Kröcher[3,4,*]

DOI: 10.1002/cite.201700146

In marine diesel engine applications, selective catalytic reduction (SCR) upstream of the turbocharger may become the preferred technology when dealing with high sulfur fuels and low exhaust gas temperatures. The target nitrogen oxide reductions in combination with minimum ammonia slip and reduced gas diffusion rates under elevated pressures require understanding of the impact of catalyst geometry on the SCR kinetics. The extent, trends, and sources for this observation are elucidated in this work by systematic testing of catalysts with equal geometry and/or intrinsic activity.

Keywords: NO_x reduction, Pressure influence, Selective catalytic reduction, V_2O_5 catalyst

Received: October 30, 2017; *accepted:* February 21, 2018

1 Introduction

Selective catalytic reduction (SCR) has proven to be an effective and cost-efficient method for removal of nitrogen oxides (NO_x) from combustion-generated exhaust gas. The importance of NO_x abatement is imminent due to the noxious nature of these emissions, which are claimed to cause more than 38 000 premature deaths globally on an annual base just because of excess NO_x emissions from on-road diesel applications [1].

In many of the densely populated coastal areas, however, contributions of passenger car NO_x emissions are smaller than the amount of NO_x emitted from marine transportation [2 – 4]. To improve this situation, the International Marine Organization's (IMO) Tier III regulation for emission control areas (ECAs) is pushing for 76.4 % NO_x reduction compared to the previous Tier II level, thereby fostering the introduction of SCR also for marine applications [5]. The USA adopted this regulation since January 01, 2016 for an ECA of 200 nautical miles off their coastlines and around their territories in the Caribbean Sea. While the impact of this unique ECA is limited so far, the introduction of a Baltic Sea and English Channel ECA for NO_x in 2021 is expected to finally lead to a strong global increase of vessels equipped with SCR systems due to the global trade pattern of merchant vessels.

The fuel sulfur content for marine vessels is regulated to 0.1 % in ECA's, the global limit outside these areas is still 3.5 %, though a reduction to 0.5 % is scheduled for 2020. However, if a sulfur oxide removal system is installed in the exhaust duct, fuel sulfur contents of 3.5 % and possibly even higher may still be used as long as the effective SO_x emissions are equivalent to the prescribed sulfur content fuel [5]. The resulting concentrations of SO_3 and H_2SO_4 in the exhaust can impose challenges for the SCR process due to the formation of ammonium bisulfate (ABS) deposits on the catalyst surface [6]. As marine engines are heavily optimized for highest fuel efficiency [7], the exhaust gas temperatures at which the SCR needs to operate are low compared to other diesel engine applications.

One solution to cope with both, potential issues due to ABS deposits and low exhaust gas temperatures, has been demonstrated to be the installation of the SCR system upstream of the turbocharger [6, 8] or, in case of two-stage charged engines, an inter-turbo setup [9, 10]. The concept of shifting parts of the exhaust gas aftertreatment system upstream of the turbocharger has been first demonstrated decades ago for three-way catalysts in automotive applications [11]. Several later studies assessed its potential for diesel oxidation catalysts and diesel particulate filters [12 – 17]. For pre-turbo SCR, there were also some earlier considera-

[1]Dr. Daniel Peitz
Winterthur Gas & Diesel, Schützenstraße 1–3, 8400 Winterthur, Switzerland.

[2]New contact details: Dr. Daniel Peitz
Hug Engineering, Im Geren 14, 8352 Elsau, Switzerland.

[3]Martin Elsener, Prof. Dr. Oliver Kröcher
oliver.kroecher@psi.ch
Paul Scherrer Institut (PSI), Bioenergy and Catalysis Laboratory, 5232 Villigen, Switzerland.

[4]Prof. Dr. Oliver Kröcher
École Polytechnique Fédérale de Lausanne (EPFL), Institute of Chemical Science and Engineering, 1015 Lausanne, Switzerland.

tions for passenger car and truck size engines [18] and larger ones as used in locomotives or marine applications [19]. For low-speed two-stroke diesel engines in the megawatt range, there were even some commercial pre-turbo SCR projects, i.e., a series of three cargo ships [20] and selected examples for stationary applications in power plants [21, 22]. If the SCR catalyst is positioned upstream of the turbo charger, it is not only exposed to higher exhaust temperatures but also to elevated exhaust gas pressures. However, there are so far only few experimental investigations elucidating the impact of increased pressure on the global SCR reaction kinetics. Actually, one of the first works claimed no net benefit for the SCR reaction at elevated pressure due to increased adsorption of NH_3 slowing down the NO_x reduction [23]. Another work relating the possible advantage of increased pressure for catalyst volume reductions and checking with experiments using different pressures at equal partial pressures clearly concluded a benefit of increased pressure for the SCR reaction, though the effect did not correspond linearly to the pressure and seemed to depend on the geometry of the catalyst [24]. These trends were later confirmed in an industry-initiated research project [25] and are today considered the reference for testing new SCR catalysts under such conditions [26, 27].

However, a systematic assessment of the impact of pressure on diffusion and, in consequence, on global reaction kinetics has not been reported so far. The effects of catalyst activity and diffusion lengths are studied in this work by choosing catalyst types of equal geometry but different activity and vice versa.

In this work, the focus is on marine SCR applications regulated by IMO Tier III, which mandates about 80 % NO_x conversion. This value is lower than in most other onshore SCR applications, however, in large marine applications, exhaust gas boilers (economizers) are typically installed downstream of the SCR system to utilize some of the exhaust heat. Furthermore, here, the potential formation of ABS deposits requires a reliable countermeasure to prevent the deposition on the heat exchanger surface, which is also known as boiler fouling. Any alteration of the temperature would compromise the boiler's efficiency; conversion of sulfur to SO_3 and H_2SO_4 is largely depending on engine operation itself and only partially on the SCR catalyst, thus, the NH_3 slip after the SCR system remains as the only ABS control parameter [28]. NH_3 slip catalysts as they are sometimes being used in automotive applications are no option for marine applications due to the high sulfur content of the marine fuels. Therefore, the SCR sizing must consider reaching the mandatory NO_x conversion rates at minimum NH_3 slip. For the experiments in this study, an industrially accepted value of no more than 2 ppm of NH_3 slip was targeted, which requires the reaction of 99.75 % of the NH_3 at the catalyst surface. Such a high value can only be reached when the impact of gas phase diffusion on the SCR converter layout is known and when it is understood how it will be affected by an increase in pressure.

2 Experimental

In this study, commercially fully extruded SCR catalysts of different geometry and composition were used. An overview of the tested catalyst types is presented in Tab. 1. Catalyst test samples with a length of 91 to 96 mm were cut out preserving the channel structure from the original 150 × 150 mm honeycomb extrudates (Fig. 1), and fitted with glass fiber mats into a round test reactor with an internal diameter of 21 mm. All calculations of catalytic activity were corrected for the actually tested sample dimensions.

Table 1. Overview of tested catalyst types. Specific surface area values are indicative only as a reference for the surface-based activity calculations.

Cell density [cpsi]	Pitch size [mm]	Specific surface area [m^2m^{-3}]	Vanadium content [mass % V_2O_5]
26	4.98	710	1.0
46	3.75	930	0.5
46	3.75	930	1.0

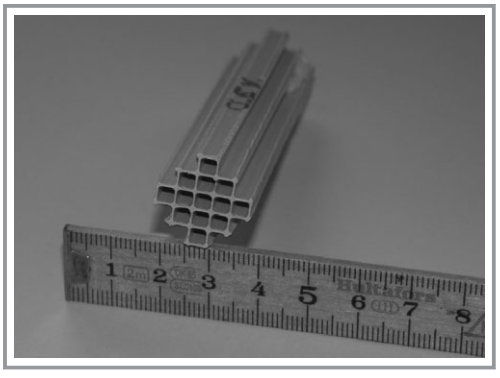

Figure 1. Picture of tested 46 cpsi 0.5 % V_2O_5 catalyst sample with 13 open cells and a length of 90 mm.

The model exhaust gas test bench consisted of electronically actuated mass flow controllers for dosing the gases nitrogen, oxygen, nitrogen oxide, and ammonia, while water was dosed pulsation-free by oxidation of corresponding amounts of hydrogen and oxygen by means of a platinum-based oxidation catalyst. All gas concentrations and flow rates were adjusted independently before the components were mixed and heated. The gas matrix contained 10 % O_2, 5 % H_2O, and balance nitrogen. For the investigations, 1000 ppm NO were used while NH_3 was dosed in the range of 0 – 1200 ppm. The gas flow rates were in the range of 90 to 400 L h^{-1} at STP to reach the specified gas hourly space velocities (GHSV). All gas transfer lines were trace-heated to 170 – 180 °C.

The reactor used for the investigations was constructed of 1.4435 stainless steel and fitted with thermocouples up- and downstream of the catalyst sample. The potential oxidation

of NO to NO_2 on the reactor walls was tested as well. The exhaust was analyzed with a Thermo Nicolet FTIR iS50 spectrometer, calibrated including the correction of cross sensitivities for all dosed exhaust gas components and possible reaction side products such as N_2O. A detailed analysis of limits of quantification and limits of determination of this method has been presented earlier [29].

The measured NO_x reduction efficiencies (= DeNOx) were calculated according to

$$\mathrm{DeNOx} = \frac{\left(c_{\mathrm{NO_{x,in}}} - c_{\mathrm{NO_{x,out}}}\right)}{c_{\mathrm{NO_{x,in}}}} \quad (1)$$

where $c_{NOx,in}$ is the concentration of NO_x in the gas upstream of the catalyst and $c_{NOx,out}$ is the concentration of NO_x in the gas downstream of the catalyst. The ratio α of dosed NH_3 to NO_x is defined as

$$\alpha = \frac{c_{\mathrm{NH_{3,in}}}}{c_{\mathrm{NO_{x,in}}}} \quad (2)$$

For calculating the volume-based reaction rate constants k_{vol} [h^{-1}] and the surface-based reaction rate constants k_{surf} [$m\,h^{-1}$], the following equations were used

$$k_{\mathrm{vol}} = -\frac{\dot{V}}{V_{\mathrm{cat}}}\ln(1-X) \quad (3)$$

$$k_{\mathrm{surf}} = -\frac{\dot{V}}{A}\ln(1-X) \quad (4)$$

where $\dot{V}$ is the gas flow rate [m^3h^{-1}], V_{cat} is the catalytic converter volume [m^3], X is the NO_x conversion, and A is the geometric surface of the catalytic converter [m^2].

2.1 Measurement Procedure

All catalysts were first tested at temperatures and pressures simulating the four two-stroke marine diesel engine load points included in the certification process (indicated by * in Tab. 2) [9, 30]. At these reference conditions, the gas flow rate at each pressure and temperature was adapted such that at an NH_3/NO ratio of α = 0.8 an ammonia concentration of 2 ± 0.2 ppm was measured downstream of the catalyst (= NH_3 slip).

At the determined gas flow, an NH_3 sweep test was conducted and plotted as an NH_3 slip/DeNOx curve ranging from α = 0 – 1.2. The same gas flow rate was used to measure the DeNOx at different temperatures while maintaining the exhaust gas pressure and NH_3 dosing rate (for each pressure, the GHSV value is constant). From the obtained NH_3 slip/DeNOx curve, the DeNOx was extracted which is reached at an NH_3 slip of 2 ppm. Thereafter, the gas flow rate was adjusted to actually reach the conditions of 2 ppm NH_3 slip at α = 0.8. The measurement points at α = 1.2, i.e., NH_3 overdosage, were used to calculate the volume or surface-based intrinsic catalytic activity rate constants k_{vol} and k_{surf} at STP, respectively.

Table 2. Overview of measurement points. GHSV values are constant for a given pressure.

T [°C]	p [bar]			
	1	2.3	3.3	4.3
475				x
450			x	x
400	x	x	x*	x*
350	x*	x*		x
300	x			x
250	x			

*Reference conditions for comparison with engine load points from the test cycle representing 25 – 100 % engine load.

3 Results and Discussion

As described in the previous section, first, the GHSV was adjusted to reach 2 ppm NH_3 slip at α = 0.8 at all reference engine load points. At each load point, the temperature was changed in steps of 50 °C according to Tab. 2 and NH_3 slip/DeNOx curves were recorded. From these curves the DeNOx at 2 ppm NH_3 slip could be extracted for all conditions. Fig. 2 displays in an overview for the 26 cpsi 1.0 % V_2O_5, 46 cpsi 1.0 %V_2O_5, and the 46 cpsi 0.5 % V_2O_5 catalysts how the

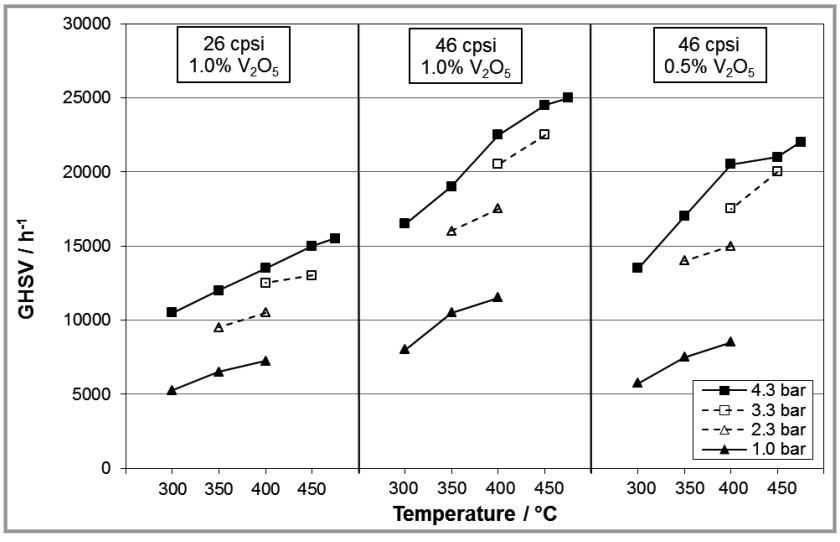

Figure 2. Comparison of GHSV values at 2 ppm NH_3 slip at α = 0.8.

GHSV needs to be adapted to maintain the desired 2 ppm NH_3 slip at $\alpha = 0.8$ when the temperature is changed in steps of 50 °C from the reference points in Tab. 2.

At atmospheric pressure ($p = 1.0$ bar), the GHSV values are comparable for the 26 cpsi 1.0 % V_2O_5 and 46 cpsi 0.5 % V_2O_5, but at elevated pressures, the 46 cpsi 0.5 % V_2O_5 catalyst is much better. It seems that at atmospheric pressure, the lower cell density, corresponding also to lower catalyst surface area, can still be compensated by higher intrinsic activity of the catalyst containing more V_2O_5. At elevated pressures, the longer mean free diffusion paths in the 26 cpsi 1.0 % V_2O_5 sample lead to significantly lower volumetric activities despite its high V_2O_5 content. Gas diffusion limitation becomes also an important factor for the 46 cpsi 0.5 % V_2O_5 sample, visible in Fig. 2 on the right. When increasing the pressure from 1.0 to 4.3 bar, the corresponding increase in residence time is not directly proportional to the increase in catalyst activity by the same factor as the gas diffusion rates decline with the increase in pressure, i.e., the higher the pressure, the more dominant the diffusion limitation. This dependency of catalyst activity from cell density and V_2O_5 content becomes even better visible when the GHSV values are plotted relative to those of the 46 cpsi 1.0 % V_2O_5 sample as reference point (Fig. 3).

The low cell density sample 26 cpsi 1.0 % V_2O_5 achieves only about 60 % of the GHSV values of the 46 cpsi 1.0 % V_2O_5 sample, which shows equal intrinsic catalytic activity independent of pressure and temperature. This ratio results from the lower geometric catalyst surface area and the increased diffusion lengths in the higher pitched catalyst structure. In case of the 46 cpsi 0.5 % V_2O_5 sample, the activity at atmospheric pressure is about 30 % lower than for 46 cpsi 1.0 % V_2O_5 with the higher intrinsic activity but same geometric structure. However, as the pressure is increased, gas diffusion becomes more dominant and the lower V_2O_5-loaded catalyst achieves almost 90 % of the activity of the reference.

The reason for the observed strong influence of diffusion on the measured activities is the requirement for minimum NH_3 downstream of the catalytic converter. Considering an example where 1000 ppm of NO have to be reduced at $\alpha = 0.8$ with 2 ppm allowed NH_3 slip means that from the dosed 800 ppm NH_3 798 ppm or 99.75 % need to diffuse to the surface to be converted. This example illustrates the strong impact of pitch size or pressure in our experiments.

To further examine the effect of pitch size and pressure, the volumetric catalyst activity rate constants at reaction conditions are compared in Fig. 4. This type of Arrhenius plot is usually only applied in case the entire catalyst mass or volume can contribute to the conversion under investigation. In this work, the measurements were conducted at 20 % excess NH_3 dosing to saturate the surface sites of the catalyst with reductant. Still, the conversion was limited by gas diffusion of NO within the honeycomb cells of the catalytic converter and possibly also within the catalyst pores. At the operating conditions, the catalyst conversion approached 100 % at high pressures and temperatures; therefore, these measurements of the activity rate constants are not applicable for deriving activation energies. Comparison of different SCR catalysts over a wide temperature window with alteration of even more parameters, such as gas concentrations, has been demonstrated earlier [31]. However, the new results provide addi-

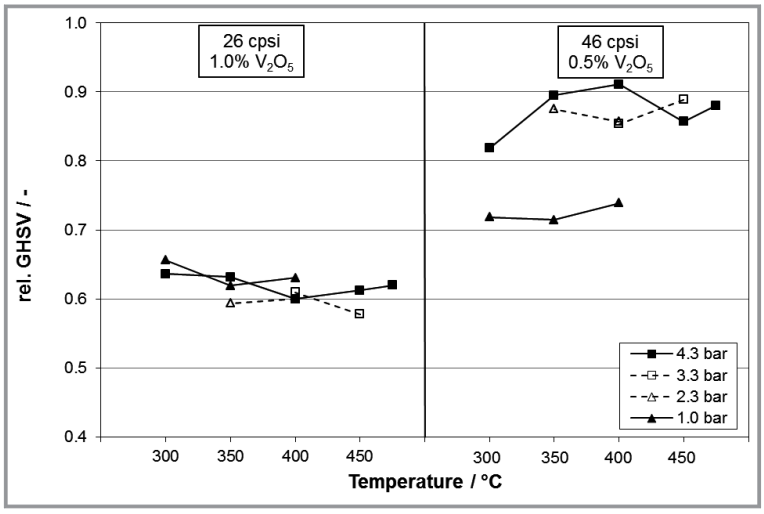

Figure 3. Relative GHSV values of 26 cpsi 1.0 % V_2O_5 and 46 cpsi 0.5 % V_2O_5 compared to 46 cpsi 1.0 % V_2O_5.

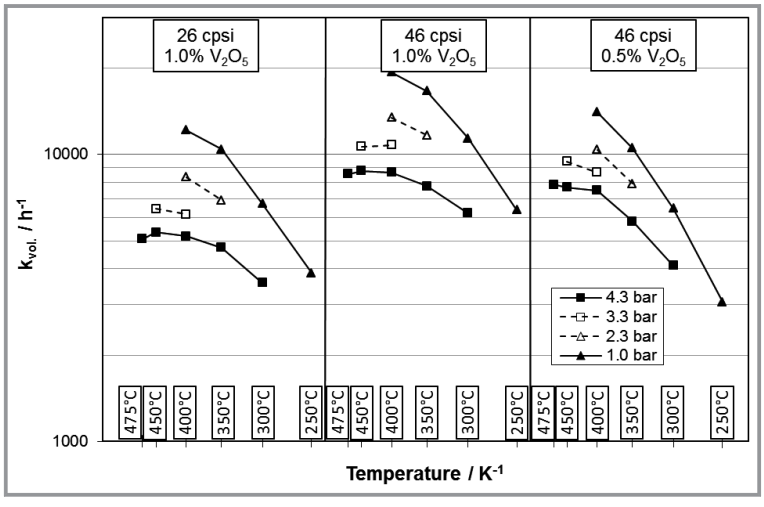

Figure 4. Volumetric rate constants of the tested catalysts at reaction conditions.

tional information how elevated pressure can enhance the volumetric rate constants at standard conditions.

Under ideal conditions without diffusion limitation, the activity curves would be expected to overlap for the different pressures. However, due to diffusion limitations at higher pressure, the highest activity is always reached at atmospheric pressure. The curves at atmospheric pressure show a typical almost linear gradient at low temperatures indicating the absence of diffusion limitation under these conditions. This means that the higher activity of 46 cpsi 1.0 % V_2O_5 sample compared to the 46 cpsi 0.5 % V_2O_5 sample under these conditions is directly related to its higher V_2O_5 content. With increasing temperature, the curves increasingly deviate from the linear behavior revealing severe diffusion limitation. As the pressure is increased, the gradients become smaller, revealing a further increasing influence of diffusion limitation on the reaction. It should be noted that increasing pressures also change the surface coverage with reactants, but earlier works indicate that the effect is rather small in comparison to the diffusion limitation [24, 25]. In this work, only the influence of pressure was studied, the influence of reactant concentrations was not considered. The influence of cell density and intrinsic activity could be disentangled by a comparison of the activities on a relative scale, again with the highest active 46 cpsi 1.0 % V_2O_5 catalyst as reference (Fig. 5).

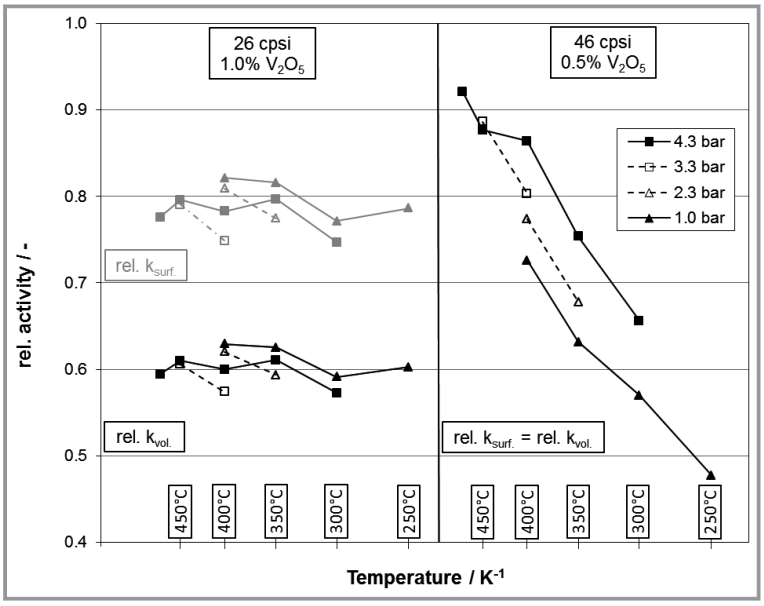

Figure 5. Relative activity rate constants of 26 cpsi 1.0 % V_2O_5 and 46 cpsi 0.5 % V_2O_5 compared to 46 cpsi 1.0 % V_2O_5.

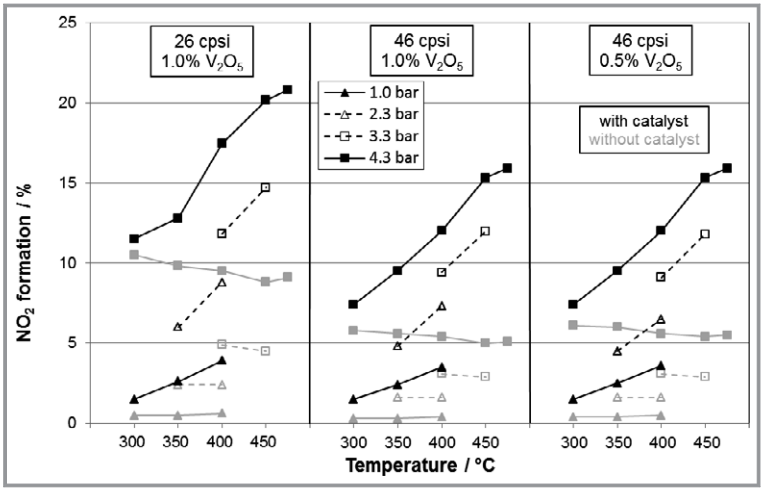

Figure 6. NO_2 formation in the empty reactor (without catalyst) and catalyst-filled reactor.

The volume-based reaction rate constant of the 26 cpsi 1.0 % V_2O_5 catalyst directly corresponds to about 60 % of the activity of the 46 cpsi 1.0 % V_2O_5 catalyst with identical vanadium content (Fig. 5). To compare these two catalysts despite their different geometric surface area, the volumetric rate constants were also converted to surface-based reaction rate constants. Consequently, the scaling factor changed to 80 %, but it remained at the same level for all measured points. The obtained curves directly reflect the different geometries of the 26- and 46-cpsi samples and their influence on the level of diffusion limitation, independent of the temperature and pressure conditions.

The right part of Fig. 5 visualizes the effect of temperature and pressure on the 46 cpsi 0.5 % V_2O_5 catalyst relative to the 46 cpsi 1.0 % V_2O_5 reference catalyst. At low temperature and pressure, i.e., at 250 °C and 1 bar, the measured DeNOx is determined by the intrinsic activity of the catalyst, which corresponds to the V_2O_5 content. As a consequence, the 46 cpsi 0.5 % V_2O_5 catalyst is less than half as active as the 46 cpsi 1.0 % V_2O_5 catalyst under these conditions. With increasing temperature, the influence of gas phase diffusion limitation is becoming dominant and the relative activities of the 46 cpsi 0.5 % V_2O_5 catalyst are steeply increasing in the direction of the reference. When the pressure is also increased, the gas phase diffusion is slowed down again, shifting the relative activity further in the direction of the reference catalyst. At 450 °C and 4.3 bar, the 46 cpsi 0.5 % V_2O_5 catalyst reaches more than 90 % of the DeNOx of the 46 cpsi 1.0 % V_2O_5 catalyst. This clearly demonstrates the impact of diffusion in high pressure SCR applications, as the catalyst with only half the intrinsic activity is catching up with the catalyst loaded with the double amount of vanadium.

The selectivity of SCR catalysts can be easily determined by analyzing the stoichiometry of the observed SCR reaction. For this purpose, the stoichiometric factor f_{stoich} was

calculated, which is defined as the ratio of consumed NH_3 and consumed NO_x:

$$f_{\text{stoich}} = \frac{c_{\text{NH}_3,\text{in}} - c_{\text{NH}_3,\text{out}}}{c_{\text{NO}_x,\text{in}} - c_{\text{NO}_x,\text{out}}} \quad (5)$$

Generally, the tested catalysts showed very small deviations from the ideal case $f_{\text{stoich}} = 1$. The largest deviations were observed at high temperatures, long residence times, and high ammonia concentrations, which facilitated side reactions of NH_3. As long as NH_3 was not dosed in excess compared to NO_x, i.e., $\alpha \leq 1$, f_{stoich} remained below 1.05 even at the highest tested temperatures and lowest gas flows. This deviation does not necessarily imply that 5 % of the dosed NH_3 were converted to side products, since some of the NH_3 could also be oxidized by oxygen to the desired product nitrogen. However, this reaction pathway caused an undesired overconsumption of NH_3, which was missing for the SCR reaction.

The formation of N_2O from NH_3 is the second most important side reaction, which has to be considered. N_2O was measured during all tests and concentrations, up to 6 ppm were found under the most challenging conditions of α = 1.2, high temperatures, and long residence times. However, N_2O emissions are no major concern even at this peak level, which is far below the industry target of 10 ppm under operating conditions [32, 33]. For comparison, EPA set a limit of 0.010 g mile^{-1} for passenger cars in the USA.

Another relevant side-product is NO_2, which is formed from NO and O_2. NO_2 is relevant for the SCR reaction as an equimolar amount of NO and NO_2 reacts much faster with NH_3 over the catalyst to nitrogen (called fast SCR) than just NO. Since the model exhaust gas contained 10 % O_2, there is an excess of oxygen for NO oxidation to NO_2, but the reaction is limited by the chemical equilibrium and reaction kinetics. The latter is a critical factor for the SCR reaction under pressure, because the increased pressure required a shift from a typical inert borosilicate or quartz glass laboratory reactor to a stainless steel pressure reactor and this material catalyzes the oxidation of NO to NO_2. Moreover, also the SCR catalysts will have a catalytic impact on NO_2 formation. Other parameters influencing the reaction are again temperature, pressure, and residence time. Fig. 6 shows the measured NO_2 yields from dosed NO at the previous test conditions for the empty reactor as well as for the reactor filled with catalyst but without NH_3 dosing.

At atmospheric pressure, the NO_2 formation from NO in the empty reactor is less than 0.5 %, while it increases to 2 – 4 % when the reactor is filled with catalyst. These concentrations are negligible for the SCR reaction, since in the presence of NH_3, NO is preferentially reacting in the SCR reaction instead of being oxidized to NO_2. NO conversion during the SCR reaction proceeds according to an exponential decline along the catalyst length, hence, the volume fraction of the catalyst which is exposed to high NO concentrations for conversion to NO_2 is very limited.

As the pressure was increased, the formation of NO_2 from NO increased significantly; for the 26 cpsi 1.0 % V_2O_5 catalyst with the lowest volumetric flow rates and consequently longest residence times, the effect was strongest. In the empty reactor, up to 11 % NO_2 formation was observed, while the 46 cpsi catalysts yielded 5 – 6 % NO_2 formation at the same pressure. Interestingly, the NO_2 concentration slightly decreased with higher temperatures in the empty reactor, following the principle of Le Chatelier with a negative temperature dependency of the NO + O_2 reaction, as expected for the uncatalyzed gas phase reaction [35]. Once a catalyst was inserted, the NO_2 formation was increasing for all tested conditions with a maximum of around 20 % conversion for the 26-cpsi catalyst with the longest residence time. This value and also the up to 15 % NO_2 formation with the 46-cpsi catalysts could impact commercial applications.

While the acceleration of the SCR reaction by enabling the fast SCR route is advantageous, NO_2 formation can be a concern for marine Tier III systems during transition in or out of an ECA. During heating up of the SCR catalyst at high engine loads (yielding high temperatures and pressures) without dosing of urea solution, the strong NO_2 formation could lead to a visible red-brownish NO_2 plume. Once the dosing is initialized, this phenomenon should cease, as the NO_2 is readily consumed in the fast SCR reaction together with NO and NH_3. The impact of NO_2 formation on the presented SCR kinetics is hard to quantify, however, for the determination of the catalyst activities at α = 1.2, the contribution is expected to be minor due to the abovementioned rapid consumption of the reactant NO in the SCR reaction.

In summary, this investigation confirmed the results from earlier studies on the effect of pressure on the SCR reaction. Although an increased absolute pressure yields inversely proportional gas volumes, longer residence times and, thus, higher conversions, this gain in activity is much less than expected due to the lower gas diffusion rates. The relative necessary catalyst volumes to reach 80 % DeNOx at no more than 2 ppm NH_3 slip can be calculated from the experimentally determined GHSV values (Tab. 3).

The ratios of experimentally determined GHSV values for 80 % DeNOx and 2 ppm NH_3 slip at 1 and 4.3 bar quantify the possible volume reduction for the different catalysts upon pressure increase. While the volume reduction is approximately 50 % for both the 26 cpsi 1.0 % V_2O_5 and the 46 cpsi 1.0 % V_2O_5, it is around 40 % for the 46 cpsi 0.5 % V_2O_5. Setting the volume of the 26 cpsi 1.0 % V_2O_5 catalyst as reference allows easy comparison of the influence of the different parameters (Tab. 3, two columns on the right). Increasing the cell density from 26 to 46 cpsi reduces the required catalyst volume to only 63 % at atmospheric pressure. Under these conditions, the intrinsic activity of the catalyst is also an important factor, as the catalyst volume increases again to 85 % of the reference catalyst upon lowering the V_2O_5 content of the 46-cpsi catalyst from 1.0 to

Table 3. Experimentally determined GHSV values for 80 % DeNOx and 2 ppm NH_3 slip at 1 and 4.3 bar absolute pressure with calculated required relative catalyst volumes.

Catalyst type	GHSV for 80 % DeNOx at 2 ppm NH_3 slip [h^{-1}]		$GHSV_{4.3bar}/GHSV_{1bar}$ [%]	Relative catalyst volume [%][a)]	
	1.0 bar	4.3 bar		1.0 bar	4.3 bar
26 cpsi 1.0 % V_2O_5	7250	13 500	54	100	54
46 cpsi 1.0 % V_2O_5	11 500	22 500	51	63	32
46 cpsi 0.5 % V_2O_5	8500	20 500	41	85	35

[a)] 26 cpsi 1.0 % V_2O_5 at 1 bar as reference.

0.5 %. In contrast to this observation, the V_2O_5 content is almost irrelevant at 4.3 bar, when diffusion rather than intrinsic catalyst activity is governing the measured DeNOx. In conclusion, the high impact of diffusion on the SCR reaction under high pressure conditions should be minimized by selecting the highest cell density still acceptable in terms of permitted pressure drop and risk management due to clogging of channels. First follow-up tests indicated more than 60 % increase in surface-based activity for an 87 cpsi 1 % V_2O_5 catalyst relative to the 26 cpsi 1 % V_2O_5 sample, which would enable even smaller catalyst volumes. The effect of external mass diffusion limitation and the possibility of mitigating its impact by higher cell densities has been described previously for 200- to 600-cpsi catalysts at 1 bar and $\alpha = 1$, which are typical conditions for SCR applications in Diesel passenger cars [36]. However, under these conditions, the impact of diffusion is lower in comparison to the present study, as the reaction is not clearly limited by one reactant and diffusion rates are higher at the lower pressure.

Clogging of channels is often difficult to predict but depends to a large extent on empirical data, because fuel quality, engine lubrication oil, combustion characteristics, and SCR reactor design can vary significantly for marine application. As indicated from the investigations, high intrinsic catalyst activity will only have a small effect on the required catalyst volume for high pressure conditions. However, if the V_2O_5 content is lowered, the conversion of SO_2 to SO_3 and H_2SO_4 can be reduced, thereby avoiding the white-blueish appearance of the exhaust from the stack ("blue plume"). The influence of high pressure conditions on the conversion of SO_2 has not been investigated in this study, for the uncatalyzed gas phase reaction, an increase in conversion is anticipated according to the principle of Le Chatelier.

Another remark concerning the pre-turbo arrangement of the SCR system is the possible impact of nonconstant flow of exhaust gas through the catalyst. The composition of exhaust gas coming from the cylinder outlets will range from scavenge air to undiluted exhaust gas due to the combustion cycle in case of a very close-coupled SCR system for low or medium speed marine engines with only a few hundred revolutions per minute (rpm). Furthermore, the gas flow rate through the catalyst is rather irregular for a pre-turbo SCR system in a single stage charged engine [37]. These conditions and their impact on the SCR process will need to be further assessed. For medium speed engines, the mixing and damping of the first turbocharger could help to improve the situation.

4 Conclusion and Outlook

The presented work highlights the impact of elevated pressure on the SCR catalyst system design by assessing the strong influence of exhaust gas pressure and catalyst geometry on the observed DeNOx performance. In particular, the SCR conditions as they are relevant for IMO Tier III applications pronounce the role of gas phase diffusion. At identical catalyst composition, the increase of the cell density from 26 to 46 cpsi results in 25 % higher surface-based reaction rate constants. Additionally, it was demonstrated that the effect of higher intrinsic catalyst activity due to increased V_2O_5 content is diminished when the catalyst operates in the gas diffusion limitation regimes as they are well known for high temperatures.

This work was funded by the European Union's Horizon 2020 research and innovation program under grant agreement No. 634135, HERCULES II.

References

[1] S. Anenberg, J. Miller, R. Minjares, L. Du, D. Henze, F. Lacey, C. Malley, L. Emberson, V. Franco, Z. Klimont, C. Heyes, *Nature* **2017**, *545 (7655)*, 467. DOI: 10.1038/nature22086

[2] J. Isakson, T. A. Persson, E. S. Lindgren, *Atmos. Environ.* **2001**, *35 (21)*, 3659. DOI: 10.1016/S1352-2310(00)00528-8

[3] P. S. Yau, S. C. Lee, J. J. Corbett, C. F. Wang, Y. Cheng, K. F. Ho, *Sci. Total Environ.* **2012**, *431*, 299. DOI: 10.1016/j.scitotenv.2012.03.092

[4] H. Saxe, T. Larsen, *Atmos. Environ.* **2004**, *38 (24)*, 4057. DOI: 10.1016/j.atmosenv.2004.03.055

[5] *Amendments to the Annex of the Protocol of 1997 to Amend the International Convention for the Prevention of Pollution from Ships, 1973, as Modified by the Protocol of 1978 Relating thereto*

(Revised MARPOL Annex VI), Resolution MEPC.176 (58), International Maritime Organization, London **2008**.
[6] K. Sandelin, D. Peitz, *CIMAC Congr. 2016*, Paper 111, Helsinki, June **2016**.
[7] www.guinnessworldrecords.com/world-records/378372-most-efficient-4-stroke-diesel-engine (Accessed on October 28, 2017).
[8] T. Fujibayashi, S. Baba, H. Tanaka, *CIMAC Congr. 2013*, Paper 29, Shanghai, May **2013**.
[9] H. Korpi, G. Hellén, L. O. Liavåg, A. Di Miceli, *CIMAC Congr. 2016*, Paper 97, Helsinki, June **2016**.
[10] M. Frobenius, C. Schmalhorst, R. Fiereder, C. Rickert, J. Dreves, M. Zallinger, *CIMAC Congr. 2013*, Paper 396, Shanghai, May **2013**.
[11] P.-F. Küper, C. Brüstle, Katalysatortechnologien für zukünftige Abgasgrenzwerte, *Wiener Motorensymp.*, Wien, April **1994**.
[12] E. Jacob, A. Döring, *21. Int. Wiener Motorensymp.*, Fortschritt-Berichte VDI, Series 12, Vol. 420, VDI-Verlag, Düsseldorf **2000**.
[13] G. Saroglia, G. Basso, M. Presti, M. Reizig, H. Stock, *SAE [Tech. Pap.]* **2002**, 2002-01-1313. DOI: 10.4271/2002-01-1313
[14] M. N. Subramaniam, C. Hayes, D. Tomazic, M. Downey, C. Brüstle, *SAE [Tech. Pap.]* **2011**, 2011-01-0299. DOI: 10.4271/2011-01-0299
[15] V. Bermúdez, J. R. Serrano, P. Piqueras, Ó. García-Afonso, *Int. J. Engine Res.* **2012**, *14 (4)*, 341. DOI: 10.1177/1468087412457670
[16] J. M. Luján, J. R. Serrano, P. Piqueras, Ó. García-Afonso, *Energy* **2015**, *80*, 599. DOI: 10.1016/j.energy.2014.05.048
[17] J. M. Luján, J. R. Serrano, P. Piqueras, Ó. García-Afonso, *Energy* **2015**, *80*, 614. DOI: 10.1016/j.energy.2014.12.017
[18] V. Joergl, P. Keller, O. Weber, K. Mueller-Haas, R. Konieczny, *SAE Int. J. Fuels Lubr.* **2009**, *1 (1)*, 82. DOI: 10.4271/2008-01-0071
[19] C. Brüstle, D. Tomazic, M. Franke, *MTZ Ind.* **2013**, *3 (1)*, 62. DOI: 10.1007/s40353-013-0073-x
[20] S. Aufdenblatten, *CARB Maritime Air Quality Technical Working Group*, Port of Oakland, CA, July **2002**. www.arb.ca.gov/ports/marinevess/presentations/072602/wartsila072602.pdf (Accessed on October 28, 2017)
[21] *SCR System for 2-Stroke MAN Diesel Engines*, Application Fact Sheet 1002, Johnson Matthey, London **2009**. www.jmsec.com/fileadmin/user_upload/pdf/application_fact_sheets/engines/afs1002_-_macau_2t.pdf (Accessed on October 28, 2017)
[22] C. Günther, R. Jürgens, K. Huber, W. Schüttenhelm, P. Reynolds, Nachrüstung einer Hochdruck-SCR an einem stationären 2-Takt-Großmotor, *4. Rostocker Grossmotorentagung*, Rostock, September **2016**.
[23] R. Bank, B. Buchholz, H. Harndorf, R. Rabe, U. Etzien, *CIMAC Congr. 2013*, Paper 188, Shanghai, May **2013**.
[24] O. Kröcher, M. Elsener, M.-R. Bothien, W. Dölling, *MTZ Worldwide* **2014**, *75 (4)*, 46. DOI: 10.1007/s38313-014-0140-x
[25] C. Hauck, T. Rammelt, *Pre-Turbo SCR: Stickoxid-Reduktion von großen Dieselmotoren durch Harnstoff-SCR vor Abgasturbolader*, Final Report, FVV Project No. 1120, Forschungsvereinigung Verbrennungskraftmaschinen (FVV), Frankfurt/Main **2013**.
[26] T. Günter, J. Pesek, K. Schäfer, A. B. Abai, M. Casapu, O. Deutschmann, J.-D. Grunwaldt, *Appl. Catal., B* **2016**, *198*, 548. DOI: 10.1016/j.apcatb.2016.06.005
[27] T. Günter, *Ph.D. Thesis*, Karlsruhe Institute of Technology **2016**.
[28] S. Matsuda, T. Kamo, A. Kato, F. Nakajima, T. Kumura, H. Kuroda, *Ind. Eng. Chem. Prod. Res. Dev.* **1982**, *21 (1)*, 48. DOI: 10.1021/i300005a009
[29] D. Peitz, A. Bernhard, M. Elsener, O. Kröcher, *Rev. Sci. Instrum.* **2011**, *82 (8)*, 084101. DOI: 10.1063/1.3617463
[30] ISO 8178-4:2017, *Reciprocating Internal Combustion Engines – Exhaust Emission Measurement – Part 4: Steady-State and Transient Test Cycles for Different Engine Applications*, 3rd ed., International Organization for Standardization, Geneva **2017**.
[31] M. Koebel, M. Elsener, *Chem. Eng. Sci.* **1998**, *53 (4)*, 657. DOI: 10.1016/S0009-2509(97)00342-4
[32] A. Vressner, P. Gabrielsson, I. Gekas, E. Senar-Serra, *SAE [Tech. Pap.]* **2010**, 2010-01-1216. DOI: 10.4271/2010-01-1216
[33] M. Kass, J. Thomas, S. Lewis, J. Storey, N. Domingo, R. L. Graves, A. Panov, P. Park, *SAE [Tech. Pap.]* **2003**, 2003-01-3244. DOI: 10.4271/2003-01-3244
[34] US Environmental Protection Agency, *Federal Register* **2010**, *75 (88)*, 25399. www.gpo.gov/fdsys/pkg/FR-2010-05-07/pdf/2010-8159.pdf (Accessed on October 28, 2017).
[35] S. S. Mulla, N. Chen, L. Cumaranatunge, G. E. Blau, D. Y. Zemlyanov, W. N. Delgass, W. S. Epling, F. H. Ribeiro, *J. Catal.* **2006**, *241 (2)*, 389. DOI: 10.1016/j.jcat.2006.05.016
[36] I. Nova, D. Bounechada, R. Maestri, E. Tronconi, A. K. Heibel, T. A. Collins, T. Boger, *Ind. Eng. Chem. Res.* **2011**, *50 (1)*, 299. DOI: 10.1021/ie1015409
[37] E. Codan, S. Bernasconi, H. Born, *CIMAC Congr. 2010*, Paper 139, Bergen, June **2010**.

